Volume 82, number 3,4 OPTICS COMMUNICATIONS 15 April 1991

Detailed characterization of Nd^{3+} doped SiO_2–GeO_2 glass fibre lasers

W.L. Barnes, P.R. Morkel and J.E. Townsend
Optical Fibre Group, The University, Southampton, SO9 5NH, UK

Received 17 September 1990

Several basic parameters of Nd^{3+} in a SiO_2–GeO_2 glass fibre have been determined. The stimulated emission cross-section for the $^4F_{3/2}\rightarrow{}^4I_{11/2}$ transition has been evaluated experimentally both by a laser technique and spectroscopically. Comparison is made between the two methods and a nonradiative decay process inferred. The efficiency of the 800 nm pump band was determined from measurements of laser slope efficiencies. Branching ratios for the different fluorescent bands have been measured and cavity losses determined.

1. Introduction

This study is concerned with the measurement of some of the basic parameters affecting laser operation of Nd^{3+} doped fibres with a SiO_2–GeO_2 glass core composition. Only operation on the $^4F_{3/2}\rightarrow{}^4I_{11/2}$ transition is considered. Of particular importance to the evaluation of a material for laser applications is the emission cross-section. Two methods are used to obtain this parameter. The first is based on studying lasing threshold as a function of output coupling. This method is particularly suited to end-pumped lasers, such as fibre lasers, relying as it does on a knowledge of the absorbed pump power [1]. The second method is spectroscopic and involves measuring the $^4F_{3/2}\rightarrow{}^4I_{11/2}$ fluorescence and determining the radiative lifetime of the transition.

2. Laser cavity method

The threshold condition for a fibre laser may be written as

$$R_1R_2(1-L_B)^2\exp(2\gamma l)=1\,, \tag{1}$$

where R_1 is the (power) reflection coefficient of the input mirror, R_2 is the reflection coefficient of the output mirror, L_B is the loss due to the fibre mirror butt, γ is the gain per unit length, l is the fibre length. The fibre is assumed to have negligible intrinsic loss at the lasing wavelength. Setting $R_1=1$, eq. (1) becomes

$$-\log_e R_2+\log_e(1-L_B)^2=2\gamma l\,. \tag{2}$$

For $L_B\ll 1$, $\log_e(1-L_B)\approx -L_B$, so that eq. (2) becomes

$$\log_e R_2-2L_B=2\gamma l\,. \tag{3}$$

The round trip gain is given by

$$2\gamma l=2\sigma\int_0^l n\,\mathrm{d}z\,, \tag{4}$$

where n is the metastable level population density. Using a two-level approximation for the lasing system, we can write the rate equation for the metastable level as

$$\mathrm{d}n/\mathrm{d}t=\eta\omega_P(n_T-n)-\omega_L n-n/\tau_f\,, \tag{5}$$

where n_T is the total population density, η is the pumping efficiency, ω_P and ω_L are the pump and stimulated rates and τ_f the fluorescent decay time. Further,

$$\omega_i=c\sigma_i\rho_i/\mu h\nu_i\,, \tag{6}$$

where σ_i, ρ_i and $h\nu_i$ are the cross-section, energy density and photon energy of the particular i. We use subscript P for the pump transition and L for the las-

ing one. The speed of light is c and μ the refractive index of the fibre core.

At threshold, $\omega_L \approx 0$ so that in equilibrium eq. (5) becomes

$$\frac{\eta c \sigma_P \rho_P}{\mu h \nu_P} (n_T - n) = \frac{n}{\tau_f} . \tag{7}$$

Assuming for the moment that the optical pump field and dopant distribution are constant across the core, we can write for a short length of fibre

$$d\rho_P/dz = -\rho_P \sigma_P (n_T - n) , \tag{8}$$

where z is the pump propagation direction along the fibre core. Combining eqs. (7) and (8) gives

$$(\eta c \tau_f / \mu h \nu_P)\, d\rho_P = -n\, dz . \tag{9}$$

Now

$$\rho_P = I_P \mu / c , \tag{10}$$

where I_P is the pump intensity at a given point. In the fibre geometry it is the mean intensity of the pump across the core that is important. Assuming now that the pump intensity distribution can be approximated by a gaussian, i.e.,

$$I_P(r) = I_P(0) \exp(-r^2/\omega_P^2) , \tag{11}$$

where r is the radial distance from the core and ω_P is the power spot size, related to the field spot size by [2] $\omega_P = \omega_0/\sqrt{2}$. The mean intensity I_m in the core is then

$$I_m = (P/\pi a^2)\, [1 - \exp(-a^2/\omega_P^2)] , \tag{12}$$

where P is the pump power at a given point along the fibre and a is the core radius. Eq. (12) thus becomes

$$I_m = P/A_{eff} , \tag{13}$$

with

$$A_{eff} = \frac{\pi a^2}{1 - \exp(-a^2/\omega_P^2)} .$$

In fact we must also take account of the overlap between the pump and lasing fields in the fibre core. Doing this we find

$$A_{eff} = \frac{\pi a^2}{1 - \exp(-a^2/\omega_P^2) \exp(-a^2/\omega_L^2)} . \tag{14}$$

We can now rewrite eq. (9) as

$$-(\eta \tau_f / A_{eff} h \nu_P)\, dP = n\, dz , \tag{15}$$

so that

$$\int_0^l n\, dz = \frac{\eta \tau_f}{A_{eff} h \nu_P} P_{abs} , \tag{16}$$

where P_{abs} is the pump power absorbed by a length l of fibre.

So far we have assumed that the dopant has a top hat distribution across the core. Measurements using wavelength dispersive X-ray analysis [3] on a fibre preform similar to that used here show that (fig. 1) $55 \pm 10\%$ of the core is occupied by dopant. The cross section we measure will thus be 55% of the true value. Bearing this in mind, we can restate the threshold condition (3) as

$$-\log_e R_2 + 2L_B = \frac{2 \times 0.55 \sigma_L \eta \tau_f P_{abs}}{A_{eff} h \nu_P} . \tag{17}$$

A plot of $\log_e R_2$ versus pump power absorbed to reach threshold will thus allow us to determine the butt loss L_B from the intercept, and the cross-section from the gradient. It is important to know the reflectivity of the output couplers (R_2) as used in the lasing cavity and this is examined in the appendix. The experimental results presented there show that the reflectivity is enhanced by an etalon formed between the cleaved fibre end and the dielectric mirror. This effect is important in that it may alter the reflectivity by up to 50%.

One particular Nd^{3+} doped fibre was used throughout, and was fabricated by the solution doping technique [4]. A relatively low dopant concen-

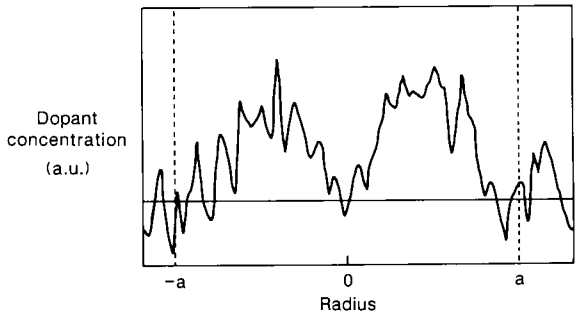

Fig. 1. Dopant distribution across the fibre core; from X-ray analysis of ref. [3].

tration of ~0.08 mole% Nd_2O_3 was chosen to avoid possible clustering of Nd^{3+} ions. GeO_2 was used to raise the core index, the resulting core composition was ~6 mole% GeO_2 in SiO_2. The numerical aperture was 0.21 and the cutoff wavelength 780 nm, thus ensuring single-mode operation at both pump and lasing wavelengths; from these parameters the core radius was found to be 1.42×10^{-6} m and the pump power spot size 1.15×10^{-6} m.

Fibre lasers were constructed by butting cleaved fibre ends up against dielectric mirrors [5]. Pump power was provided by a single stripe laser diode operating at 826 nm. Sufficient fibre (~2 m) was used to absorb >99% of the pump light. The launched pump power was determined by a multiple cut back technique.

A typical lasing characteristic is shown in fig. 2. To within experimental error, all characteristics were linear well above threshold, indicating that the laser is effectively homogeneously broadened (discussed later). It is possible to define two values of the threshold. One is given by the onset of relaxation oscillations, the other by extrapolating the characteristic (using a linear fit) to zero output power. Determining thresholds with these two definitions for many lasers allows us to plot $\log_e R_2$ versus P_{abs}, as shown in fig. 3. We see that, whilst the gradient for the two classes of threshold are similar, the intercepts are significantly different, L_B being $2.5\pm1\%$ for the relaxation oscillation set and ~12% for the fitted set. Previous measurements on butt losses [6,7] indicate 2.5% to be quite reasonable whilst 12% would be excessive; thus the onset of relaxation oscillations is taken as the threshold condition. To extract the cross section from the gradient obtained from fig. 3 we still have to determine both η and τ_f, eq. (17).

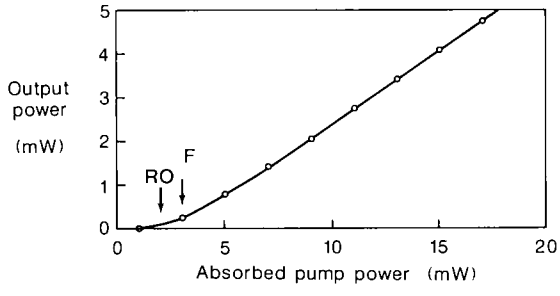

Fig. 2. Experimental lasing characteristic for an output coupler of $R=70\%$. Threshold as defined by the onset of relaxation oscillations (RO) and by fitting (F) the characteristic are shown.

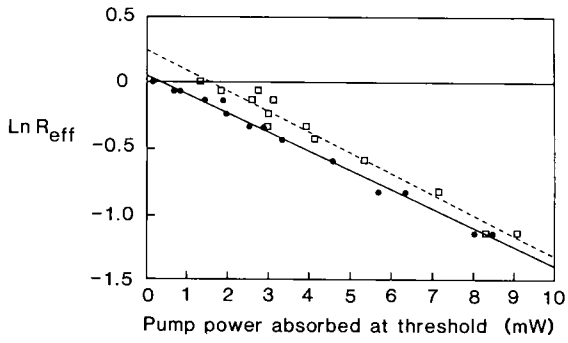

Fig. 3. Fibre laser threshold versus $\log_e R$ for fitted threshold (open data), and relaxation oscillations (solid data).

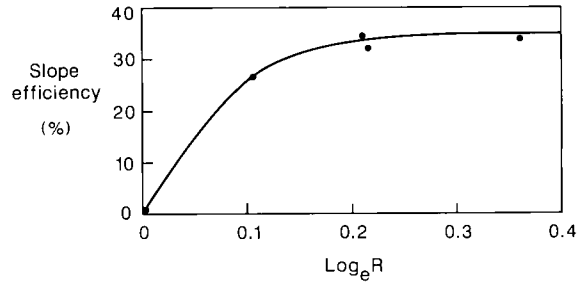

Fig. 4. Slope efficiency (with respect to absorbed pump power) versus $\log_e R$. (Note that the slope efficiency falls to half its maximum value when the output coupling equals the cavity loss, ~5%, in good agreement with that found by other methods, see text.)

The pumping efficiency η may be derived from the slope efficiency of the fibre laser output. Experimental data for slope efficiency (with respect to absorbed pump power) is shown in fig. 4. Assuming small output coupling the slope efficiency δ may be written as

$$\delta=\eta\beta\left(\frac{T}{T+L_i}\right)\frac{\nu_L}{\nu_P}, \qquad (18)$$

where β is the signal/pump modal overlap [8,9] and is calculated to be 0.96, $T=1-R_2$ and L_i is the intrinsic cavity loss. Restricting ourselves to $T\leqslant30\%$ and using $L_i=2\times L_B$ ($L_B=2.5\%$), we find $\eta=0.61^{+0.02}_{-0.06}$.

We note that our highest slope efficiencies, $\leqslant40\%$,

are lower than some of those obtained in other reports based on Al_2O_3–SiO_2 ($\sim 59\%$) [10] and SiO_2 ($\sim 51\%$) [11] glass. It has been found [12] that colour centres reduce the fluorescence conversion efficiency. It is known [13] that GeO_2–SiO_2 glass formed by the MOCVD process used in fibre fabrication process contains colour centres. This may explain the lower slope efficiencies we found in this work.

The fluorescent decay time was found by monitoring the fluorescent intensity as a function of time. The fibre was pumped with a dye laser operating at 826 nm, an acousto-optic modulator being used to pulse the pump light entering the fibre. As is typical of Nd^{3+} in glass hosts [14], the decay is found to be slightly nonexponential, as shown in fig. 5. The fluorescent decay time ranges from 430 to 530 μs across the time scale of fig. 5. For this nonexponential decay we define an equivalent decay rate

$$\tau_f = \int_0^\infty \frac{A(t)}{A(0)}\,dt\,, \tag{19}$$

where $A(t)$ is the fluorescent intensity at time t. With this definition we find the equivalent decay rate to be 460 ± 15 μs.

Combining all this information we calculate the lasing cross section to be

$$\sigma_L = (0.75 \pm 0.2) \times 10^{-24}\ \mathrm{m}^2\,.$$

It is also of interest to examine the output spectrum of the free running fibre laser. Looking first at the peak wavelength, a typical output spectrum for the laser is shown in fig. 6. The spiky nature of the output is believed to be due to etalon effects in the mirrors used to form the cavity. Whilst the spectrum broadens as the pump power is increased, fig. 7, the peak wavelength remains constant at 1.088 μm [15].

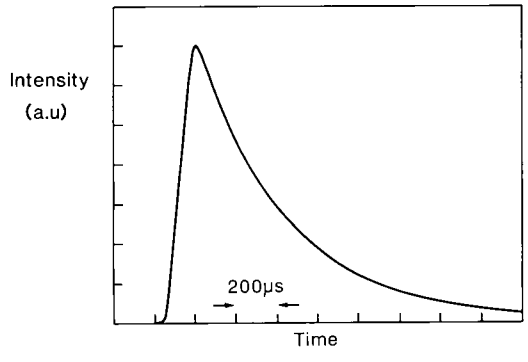

Fig. 5. Experimental decay of $^4F_{3/2} \rightarrow {}^4I_{11/2}$ fluorescence.

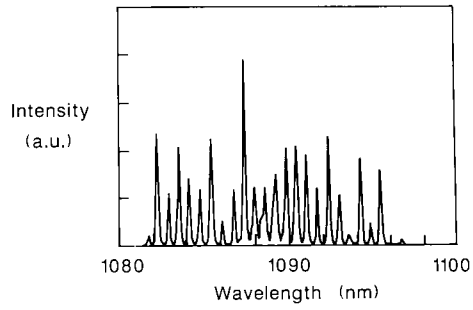

Fig. 6. Fibre laser output spectrum.

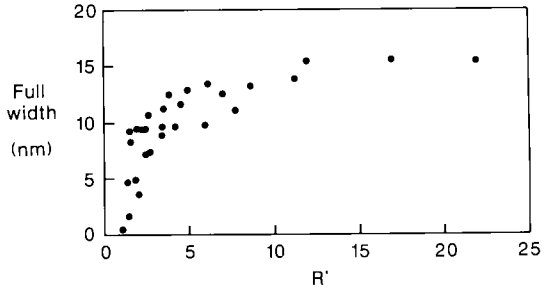

Fig. 7. Fibre laser bandwidth versus R', where R' is the ratio of pump power to threshold pump power. These data are a compilation of those obtained on many cavities.

3. Spectroscopic method

The second method of determining the cross section uses information obtained from the fluorescence spectrum. Assuming any excited state absorption to be minimal, the cross section may be calculated from the Fuchtbauer–Ladenberg equation [14]

$$\sigma_L = \frac{\lambda^4}{\tau_{spont} \cdot 8\pi c \mu^2\, \Delta\lambda_{eff}}\,, \tag{20}$$

where λ is the peak wavelength, $\Delta\lambda_{eff}$ is the effective linewidth of the transition, τ_{spont} is the radiative decay time of the transition.

The branching ratios for the three transitions, $^4F_{3/2} \rightarrow {}^4I_{9/2}$ (940 nm), $^4F_{3/2} \rightarrow {}^4I_{11/2}$ (1090 nm), $^4F_{3/2} \rightarrow {}^4I_{13/2}$ (1350 nm), were found by measuring the fluorescent output for each, care being taken to ensure no re-absorption for the 940 nm transition. The result of many such measurements gave the branching ratios as [16] 0.56:10.4:10.04. We can now use the measured value of the fluorescent decay time, 460 μs, to calculate the spontaneous rates (assuming no nonradiative decay),

$\tau_{940\,\mathrm{nm}} = 820 \pm 70\ \mu\mathrm{s}$,

$\tau_{1090\,\mathrm{nm}} = 1150 \pm 170\ \mu\mathrm{s}$,

$\tau_{1350\,\mathrm{nm}} = 11500 \pm 500\ \mu\mathrm{s}$.

The fluorescent output spectrum of the $^4F_{3/2} \rightarrow {}^4I_{11/2}$ transition, pumped at 825 nm, is shown in fig. 8. (N.B. The fluorescence spectrum varies with pump wavelength [17].) The effective width, $\Delta\lambda_{\mathrm{eff}}$, may be defined by [18]

$$I_{\mathrm{pk}}\,\Delta\lambda_{\mathrm{eff}} = \int_0^\infty I_\lambda\,\mathrm{d}\lambda\,. \tag{21}$$

From fig. 8 we find $\Delta\lambda_{\mathrm{eff}} = 57 \pm 3$ nm. From eq. (20) we may now calculate the cross-section; we find

$\sigma_{\mathrm{L}} = (1.3 \pm 0.2) \times 10^{-24}\ \mathrm{m}^2$.

4. Discussion

The cross-sections derived by the two techniques are different and two possibilities arise.

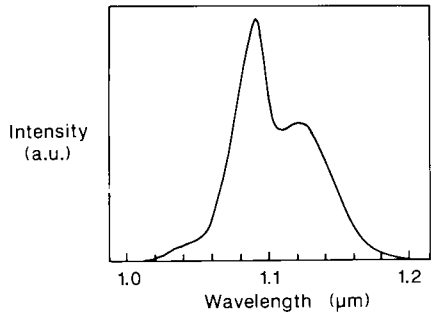

Fig. 8. Fluorescent spectrum of the $^4F_{3/2} \rightarrow {}^4I_{11/2}$ transition in a silica/germania doped fibre pumped at 825 nm.

(i) The formulae used to derive the cross-sections are inappropriate, i.e., the assumptions made are not strictly applicable to this case. A possible problem is the assumption of homogeneous behaviour, particularly important in the derivation of eq. (17). [Although there is considerable inhomogeneous broadening from the glass, this is small compared to the effect of the Stark splitting.] The homogeneous and inhomogeneous linewidths have been estimated for a silicate glass to be 60 and 120 cm^{-1} respectively [19]. If these linewidths apply to our system then the laser is not purely homogeneous, but, according to Casperson [20], can be considered as being effectively homogeneous in character.

(ii) The difference is real. In this case, since the laser cavity measurement gives a lower cross-section, a nonradiative decay process is indicated.

If we assume the second of these to be the case then we can calculate the nonradiative decay rate and find it to be $\tau_{\mathrm{NR}} = 1100^{+3200}_{-400}$ μs. Assuming that the highest-frequency phonons in our GeO_2–SiO_2 glass are due to Si–O–Si stretching mode vibrations, then the multiphonon decay rate is expected to be ~5000 μm [21]. This is close to our upper limit for τ_{NR}, indicating that nonradiative decay may well be present. Further, we can predict from the cross-section difference that the radiative lifetime is in the range 500–1300 μs and that as a result the radiative quantum efficiency ($\tau_{\mathrm{fl}}/\tau_{\mathrm{rad}}$) is 0.6 ± 0.3. The resulting fluorescence conversion efficiency is thus 0.35 ± 0.2; this compares with 0.43 ± 0.04 found for silicate glass [22].

There appears to be no previous work on Nd^{3+} doped GeO_2–SiO_2 glass. However, Nd^{3+}–SiO_2 has been studied [14,23], and spectroscopically there appears to be little difference. The peak emission wavelength for both is 1.09 μm (the addition of other glass formers to silica such as Al_2O_3 or P_2O_5 all significantly alter the peak wavelength), the linewidth is comparable too [23] and so is the fluorescent decay time. As a result we might expect the emission cross-section in GeO_2–SiO_2 to be the same as that in pure SiO_2. However, in ref. [14] the cross-section is reported as 1.9×10^{-24} m^2. This was derived spectroscopically and so should be compared to our spectroscopic value of 1.3×10^{-24} m^2. The difference may be attributed to the values of fluorescent linewidth and branching ratio used in ref. [14] (their branch-

ing ratio was calculated rather than measured). Our values for these parameters are different from ref. [14], but agree with those of ref. [23]. It therefore seems that the cross-section given in ref. [14] is in error, even if nonradiative decay is ignored.

In summary, we have determined the stimulated emission cross-section of Nd^{3+} in GeO_2–SiO_2 by two methods and obtained slightly different results from each. They are $(0.75\pm0.2)\times10^{-24}$ m^2 and $(1.3\pm0.2)\times10^{-24}$ m^2 by laser and spectroscopic techniques, respectively. The nonradiative decay rate implied by this difference is not inconsistent with that expected from the maximum phonon energies available in the glass and indicates that the cross-section difference is due to the presence of nonradiative decay.

Acknowledgements

This work was supported by the Amoco Technology Company. The authors would like to acknowledge the assistance of I.M. Jauncey in this work.

Appendix A

An accurate knowledge of the reflectivity is important in order to apply the laser cavity technique to cross-section determination. In the fibre laser a cleaved fibre end is butted close to the surface of the mirror. Two possibilities arise. Firstly the fibre may be in optical contact with the mirror and the reflectivity will be close to that measured in air. Secondly, the fibre end face may be a small distance from the mirror. A small gap between the fibre and the mirror results in the formation of a Fabry–Pérot cavity whose effect may be to enhance the reflectivity of the mirror. In practice a fibre laser in which the ends are butted to mirrors is "tweaked" to provide a minimum threshold. This is done by holding the fibre in contact with the mirror and then moving the fibre in the plane of the mirror. As a result the fibre is always in contact with the mirror and a gap can only be achieved if the fibre is tilted with respect to the normal axis of the mirror. Whilst such a tilt results in extra coupling losses [24], the gap will enhance the reflectivity and the net effect may be to reduce the laser threshold.

The nine mirrors used for Nd^{3+} fibre laser experiments were all examined. The mirrors were measured with a spectrophotometer to determine their "standard" reflectivity. To simulate the conditions applying to a fibre laser the experiment in fig. 9 was set up. A white light source produced the signal and a monochromator was used to provide an optical bandwidth of ~15 nm, centred at 1088 nm (the Nd^{3+} lasing wavelength). The light exiting the monochromator was launched into one arm of a fibre coupler. One of the output ports of the coupler was butted against the mirror, the other being terminated in index matching oil. The remaining arm of the coupler was used to monitor the reflected intensity.

Fibre cleaves were examined interferometrically and only those flat to two optical fringes or less were used as would be the case in a fibre laser experiment. For each mirror the butt between the fibre and mirror was adjusted to provide maximum reflectivity, just as it would in a laser experiment.

Theoretical analysis gives a simple formula for the maximum reflectivity obtainable with a small gap between fibre and mirror [25]. This reflectivity is given by

$$R_{\text{eff}}=[(\sqrt{r}+\sqrt{R})/(1+\sqrt{rR})]^2,$$

where r is the Fresnel reflection coefficient of the bare fibre end, R is the reflectivity of the mirror, as measured by the spectrophotometer.

Comparison of this theory with the experimental data is presented in fig. 10. The good agreement indicates that a gap does exist between fibre and mirror, produced whilst maintaining part of the fibre in contact with the mirror. The resulting enhancement can be up to 50% of the original mirror reflectivity. The minimum gap that still produces maximum en-

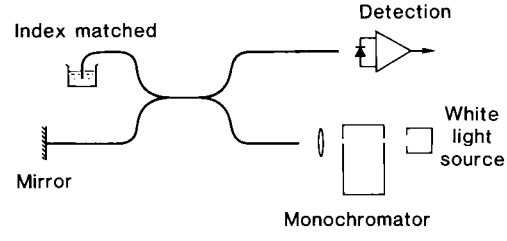

Fig. 9. Apparatus used for reflectivity measurements.

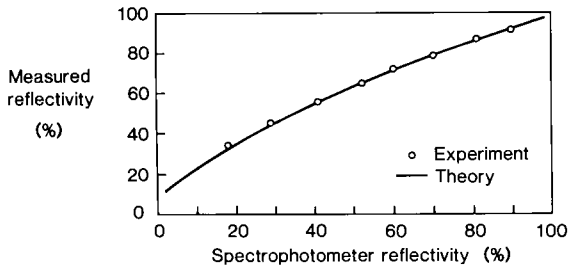

Fig. 10. Measured reflectivity (crosses) and theory (see appendix).

hancement of the reflectivity is ~ 0.2 μm. Such a gap would cause a tilt of $\sim 0.2°$ and a resultant coupling loss [24] of $\sim 1\%$. Over most of the reflectivity range examined this loss is considerably smaller than enhancement in reflectivity due to the cavity so formed.

References

[1] M. Birnbaum and J.A. Gelbwachs, J. Appl. Phys. 43 (1972) 2335.
[2] E. Desurvire and J.R. Simpson, J. Lightwave Technol. 7 (1989) 835.
[3] Murano Glass Institute, Venice, Italy, private communication;
see also B.J. Ainslie, S.P. Graig, S.T. Davey and B. Wakefield, Mater. Lett. 6 (1988) 139.
[4] J.E. Townsend, S.B. Poole and D.N. Payne, Electron. Lett. 23 (1987) 329.
[5] R.J. Mears, L. Reekie, S.B. Poole and D.N. Payne, Electron. Lett. 21 (1985) 738.
[6] P.R. Morkel, M.C. Farries and D.N. Payne, Electron. Lett. 24 (1988) 92.
[7] D.C. Hanna, P.G. Smart, P.J. Suni, A.I. Ferguson and M.W. Phillips, Optics Comm. 68 (1988) 128.
[8] W.P. Risk, J. Opt. Soc. Am. B 5 (1988) 1412.
[9] K. Kubodera and K. Otsuka, J. Appl. Phys. 50 (1979) 653.
[10] K. Lui, M. Digonnet, K. Fesler, B.Y. Kim and H.J. Shaw, Electron. Lett. 24 (1988) 838.
[11] M. Shimizu, H. Suda and M. Horiguchi, Electron. Lett. 23 (1987) 768.
[12] D.P. Devor, L.G. DeShazer and R.C. Pastor, IEEE J. Quantum Electron. QE-25 (1989) 1863.
[13] F.J. Frieble and D.L. Griscon, Mater. Res. Symp. Proc. 61 (1986) 319.
[14] R.R. Jacobs and M.J. Weber, IEEE J. Quantum Electron. QE-12 (1976) 102.
[15] J. Stone and C.A. Burrus, Appl. Phys. Lett. 23 (1973) 388.
[16] I.M. Jancey, Diode-pumped active fibre devices, PhD Thesis, Univ. of Southampton, UK (1989).
[17] P.R. Morkel, Characterization of neodymium doped fibre lasers, PhD Thesis, Univ. of Southampton, UK (1990).
[18] J.G. Edwards, Brit. J. Appl. Phys. (J. Phys. D) 1 (1968) 449.
[19] J.M. Pellegrino, W.M. Yen and M.J. Weber, J. Appl. Phys. 51 (1980) 6332.
[20] L.W. Casperson, Appl. Optics 19 (1980) 422.
[21] C.B. Layne, W.H. Lowdermilk and M.J. Weber, IEEE J. Quantum Electron. QE-11 (1975) 798.
[22] L.G. DeShazer and L.G. Komai, J. Opt. Soc. Am. 55 (1965) 940.
[23] K. Arai, H. Namikawa, K. Kumata, T. Honda, Y. Ishii and T. Handa, J. Appl. Phys. 59 (1986) 3430.
[24] D. Marcuse and J. Stone, J. Lightwave Technol. 4 (1986) 377.
[25] D. Findlay and R.A. Clay, Phys. Lett. 20 (1966) 277.